ACCURATE CONSTITUTIVE RELATIONS FOR SHOCK WAVE STRUCTURES IN GASES

M. H. LAKSHMINARAYANA REDDY & S. KOKOU DADZIE
School of Engineering and Physical Sciences, Heriot-Watt University, Scotland, UK

ABSTRACT

Predicting accurately shock wave structures in gases using an appropriate hydrodynamic model is still a challenge in extended hydrodynamic model development in rarefied gases. In this paper, we identified constitutive equations that provide better agreement for the prediction of shock structure in a monatomic gas in the Mach number range 1.3–4. The results obtained show an improvement upon those obtained previously in the bi-velocity hydrodynamics and are more accurate than in the hydrodynamic models from expansions method solutions to the Boltzmann equation.

Keywords: shock waves, compressible flows, rarefied gas flows, constitutive relations, Navier–Stokes equations, volume/mass diffusion.

1 INTRODUCTION

Shock wave structure description is one of the best-known example of a simple highly non-equilibrium compressible flow problem where large gradients of hydrodynamic fields are present [1]–[8]. Shock structure problem serves as a standard benchmark problem for testing the capability (validity) and accuracy of different hydrodynamics and extended hydrodynamic fluid flow models and provides few advantages in its numerical simulations: (i) flow is one-dimensional and steady state; (ii) no solid boundaries; and (iii) the upstream and downstream states are in equilibrium and are connected by simple relations (the Rankine–Hugoniot relations). Theoretical and numerical studies of the shock structure based on the classical Navier–Stokes (NS) equations are described in the literature [1], [2], [9]–[12]. In addition, shock density measurements have been carried out and reported for argon and nitrogen gases with Mach number that ranges from supersonic to hypersonic [13], [14]. Eventually, it has been recognized that shock structures in monatomic gases are not well described by the Navier–Stokes theory. The shock thickness predicted is too small compared to experiments for Mach numbers larger than approximately 1.5 (see. Fig. 1). The failure of the equations in a shock structure description may be tied up to the basic assumptions such as linear constitutive relations represented by Newton's law of viscosity and Fourier's law of heat conduction used in closing the system [15] and/or breakdown of continuum assumption as the mean free path becomes comparable to the characteristic length scale of the system.

The principal parameter which is often used to classify the non-equilibrium state of a gas flow is the Knudsen number, Kn, and is defined as the ratio of the mean free path of the gas molecules to the characteristic length of the flow system. Kn characterizes the gas rarefaction which means that it measures departure from the local equilibrium. Continuum assumption is valid for vanishing Knudsen numbers where the gas can be assumed to undergo a large number of collisions over the typical length scale. As Kn increases the notion of the gas as a continuum fluid becomes less valid and the departure of the gas from the local thermodynamic equilibrium increases. Therefore, the range of use of the continuum-equilibrium assumption is limited and confined to $\mathrm{Kn} \lesssim 0.01$. Generally, the shock macroscopic parameter called the inverse shock thickness is related to the Knudsen number and typically falls between ≈ 0.2 and ≈ 0.3 [6] (which is also evident from Fig. 1). Clearly, the range of Kn found in the shock problem is beyond the classical continuum-Kn regime and falls into the so-called

'intermediate-Kn' regime ($0.01 \lesssim \mathrm{Kn} \lesssim 1$). Deriving appropriate continuum hydrodynamic models or improving the range of applicability of the existing ones (the Navier–Stokes equations) beyond their limits into the so-called 'intermediate-Kn' regime ($0.01 \lesssim \mathrm{Kn} \lesssim 1$) is still a critical area of research.

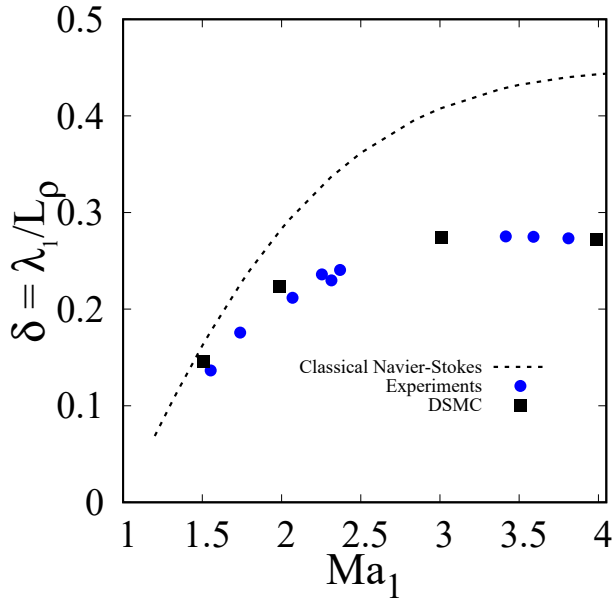

Figure 1: Variation of dimensionless inverse shock thickness (δ) verses upstream Mach number Ma_1 for a monatomic argon gas. Experimental data extracted from Alsmeyer [13] and DSMC data extracted from Lumpkin and Chapman [16].

Recently, the authors reinterpreted shock structure predictions of the classical Navier–Stokes equations using a change of velocity variable [17]–[19]. The results on the shock density profiles and shock thicknesses better agreed with the experimental data. However, the procedure predicted very less values for density asymmetry factor. The present work expands on this previous work to identify constitutive relations with a full assessment of the shock structure problem.

The paper is organized as follows. In Section 2 a brief overview of the classical Navier–Stokes equations for compressible flows and the modified constitutive relations are presented. In Section 3 the modified Navier–Stokes equations are considered subject to shock structure problem in monatomic argon gas. The detail of the formulation of the problem and numerical procedure are then provided. Section 4 is completely devoted to analysis based on comparison of shock macroscopic profiles and different shock macroscopic parameters with available experiments and other simulation data. Finally, conclusions are drawn in Section 5.

2 THE CONTINUUM FLOW EQUATIONS: MODIFIED CONSTITUTIVE RELATIONS

The standard continuum hydrodynamic equations are a differential form of three classical conservation laws, namely, mass, momentum and energy conservation laws that govern the

motion of a fluid. Here, we adopt the classical conservation equations in an Eulerian reference frame as given by:

mass balance equation

$$\frac{\partial \rho}{\partial \mathrm{t}} + \nabla \cdot [\rho \, \mathrm{U}] = 0, \tag{1}$$

momentum balance equation

$$\frac{\partial \rho \, \mathrm{U}}{\partial \mathrm{t}} + \nabla \cdot [\rho \, \mathrm{U} \otimes \mathrm{U} + \mathrm{p} \, \mathbf{I} + \mathbf{\Pi}] = 0, \tag{2}$$

energy balance equation

$$\frac{\partial}{\partial \mathrm{t}} [\frac{1}{2} \rho \, \mathrm{U}^2 + \rho \, \mathbf{e}_{\mathrm{in}}] + \nabla \cdot [\frac{1}{2} \rho \, \mathrm{U}^2 \, \mathrm{U} + \rho \, \mathbf{e}_{\mathrm{in}} \, \mathrm{U} + (\mathrm{p} \, \mathbf{I} + \mathbf{\Pi}) \cdot \mathrm{U} + \mathbf{q}] = 0, \tag{3}$$

where ρ is the mass-density of the fluid, U is the flow mass velocity, p is the hydrostatic pressure, $\mathbf{e}_{\mathrm{in}}$ is the specific internal energy of the fluid, $\mathbf{\Pi}$ is the shear stress tensor, $\mathbf{I}$ is the identity tensor and $\mathbf{q}$ is the heat flux vector. All these hydrodynamic fields are functions of time t and spatial variable $\mathbf{x}$. Additionally, ∇ and $\nabla\cdot$ denote the usual spatial gradient and divergence operators, respectively, and $\mathrm{U} \otimes \mathrm{U}$ represents the tensor product of two velocity vectors. Expression for the specific internal energy is given by, $\mathbf{e}_{\mathrm{in}} = \mathrm{p}/\rho(\gamma - 1)$ with γ being the isentropic exponent. The constitutive models for the shear stress $\mathbf{\Pi}$ and the heat flux vector $\mathbf{q}$ as due to the Newton's law and the Fourier's law, are given respectively by,

$$\mathbf{\Pi}^{(\mathrm{NS})} = -2 \, \mu \left[\frac{1}{2} (\nabla \mathrm{U} + \nabla \mathrm{U}') - \frac{1}{3} \mathbf{I} \, (\nabla \cdot \mathrm{U}) \right] = -2 \, \mu \, \overset{\circ}{\overline{\nabla \mathrm{U}}}, \quad \mathbf{q}^{(\mathrm{NS})} = -\kappa \, \nabla \mathrm{T}, \tag{4}$$

where $\nabla \mathrm{U}'$ represents the transpose of $\nabla \mathrm{U}$. Coefficients μ and κ are the dynamic viscosity and the heat conductivity, respectively.

The eqns (1)–(4) is the well known and widely accepted conventional fluid flow hydrodynamic model for a viscous and heat conducting fluid. In the limit of vanishing viscous and heat conducting terms, the model reduced to the simple gas dynamics model known as Euler equations, which are used to model inviscid and non-diffusive flows. In the present study, to investigate our shock structure problem we adapt constitutive equations from previous studies (Dadzie [20], Brenner [21]):

$$\mathbf{\Pi} = -2 \, \mu \, \overset{\circ}{\overline{\nabla \mathrm{U}}} - 2 \, \mu \, \overset{\circ}{\overline{\nabla \mathrm{J_D}}}, \quad \mathbf{q} = -\kappa \, \nabla \mathrm{T} - \frac{\gamma}{(\gamma - 1)\mathrm{Pr}} \, \mathrm{p} \, \mathrm{J_D}, \tag{5}$$

where Pr is the Prandtl number and is a dimensionless number defined as the ratio of momentum diffusivity to thermal diffusivity, $\mathrm{J_D} = \kappa_{\mathrm{m}} \nabla \ln \rho$ and κ_{m} is an additional transport coefficient, the molecular diffusivity coefficient and is here related to the kinematic viscosity coefficient through the following relation:

$$\kappa_{\mathrm{m}} = \kappa_{\mathrm{m_0}} \frac{\mu}{\rho}, \qquad \text{where } \kappa_{\mathrm{m_0}} \text{ is a positive constant.} \tag{6}$$

It is note worthy to point here that constitutive relations given in eqn (5) are formally those proposed in Dadzie [20], Brenner [21] and used in Greenshields and Reese [6]. The only main difference in the current expression being the additional factor of $\gamma/((\gamma - 1)\mathrm{Pr})$ in the heat flux relation. In the following sections, we reveal that these constitutive relations show the best prediction of the shock profile in a monatomic argon gas.

3 THE SHOCK STRUCTURE PROBLEM IN A MONATOMIC GAS: FORMULATION AND NUMERICAL PROCEDURE

The evolution of a monatomic ideal gas flow is determined by the density ρ, the velocity U and the temperature T at any point in space and time. Its pressure p obeys the perfect gas law,

$$\mathrm{p} = \rho \mathbf{R} \mathrm{T}, \tag{7}$$

where $\mathbf{R} = \mathrm{k_B}/\mathrm{m}$ is the specific gas constant with $\mathrm{k_B}$ and m being the Boltzmann constant and the molecular mass, respectively. In terms of the specific heat at constant pressure, $\mathrm{c_p}$, and constant volume, $\mathrm{c_v}$, a monatomic ideal gas is characterized by,

$$\mathrm{c_p} = \frac{\gamma}{(\gamma - 1)}\mathbf{R}, \qquad \mathrm{c_v} = \frac{1}{(\gamma - 1)}\mathbf{R}, \tag{8}$$

such that the ratio of c_p to c_v, called the isentropic constant γ, is equal to $5/3$.

We consider a planar shock wave propagating in the positive x-direction which is established in a flow of a monatomic gas. For this one-dimensional flow problem, all hydrodynamic variables are functions of a single spatial coordinate x and time t; the system is assumed to be uniform (having no gradients) and infinite along the y- and z-directions. The flow velocity and heat flux in the x-direction are denoted by $\mathrm{u}(\mathrm{x},\mathrm{t})$ and $\mathrm{q}(\mathrm{x},\mathrm{t})$, respectively, and are zero in the two remaining (y and z) orthogonal directions. It is straightforward to verify that the stress tensor has only one non-zero component, the longitudinal stress which can be expressed as,

$$\Pi_{\mathrm{xx}} = -\frac{4}{3}\mu\frac{\partial \mathrm{u}}{\partial \mathrm{x}} - \frac{4}{3}\frac{\mu\,\kappa_{\mathrm{m}}}{\rho}\frac{\partial^2 \rho}{\partial \mathrm{x}^2} + \frac{4}{3}\frac{\mu\,\kappa_{\mathrm{m}}}{\rho^2}\left(\frac{\partial \rho}{\partial \mathrm{x}}\right)^2 \equiv \Pi, \tag{9}$$

and the constitutive relation for the heat flux is,

$$\mathrm{q} = -\kappa\frac{\partial \mathrm{T}}{\partial \mathrm{x}} - \frac{\mathrm{c_p}}{\mathrm{Pr}}\kappa_{\mathrm{m}}\,\rho\,\mathrm{T}\frac{\partial \ln \rho}{\partial \mathrm{x}}. \tag{10}$$

With the above definitions, the one-dimensional reduced balance equations for the modified Navier–Stokes model can be written in 'conservative' form:

$$\frac{\partial \rho}{\partial \mathrm{t}} + \frac{\partial}{\partial \mathrm{x}}(\rho\,\mathrm{u}) = 0, \tag{11}$$

$$\frac{\partial}{\partial \mathrm{t}}\Big(\rho\,\mathrm{u}\Big) + \frac{\partial}{\partial \mathrm{x}}\Big(\rho\,\mathrm{u}^2 + \rho\,\mathbf{R}\,\mathrm{T} + \Pi\Big) = 0, \tag{12}$$

$$\frac{\partial}{\partial \mathrm{t}}\left(\frac{1}{2}\rho\,\mathrm{u}^2 + \mathrm{c_v}\,\mathrm{T}\right) + \frac{\partial}{\partial \mathrm{x}}\left(\frac{1}{2}\rho\,\mathrm{u}^3 + \mathrm{c_p}\,\rho\,\mathrm{T}\,\mathrm{u} + \Pi\,\mathrm{u} + \mathrm{q}\right) = 0. \tag{13}$$

The one-dimensional classical Navier–Stokes system is obtained by setting $\kappa_{\mathrm{m}} = 0$ in the constitutive relations of longitudinal stress and heat flux, i.e., in eqns (9) and (10), respectively. The corresponding Euler system is then obtained by setting $\Pi = 0$ and $\mathrm{q} = 0$ in eqns (11)–(13).

We denote the upstream ($\mathrm{x} \to -\infty$) and downstream ($\mathrm{x} \to \infty$) conditions of a shock, located at $\mathrm{x} = 0$, by a subscript 1 and 2, respectively. That is the upstream and the down stream equilibrium states are characterised by $(\rho_1, \mathrm{u}_1, \mathrm{T}_1)$ and $(\rho_2, \mathrm{u}_2, \mathrm{T}_2)$, respectively. Across a shock, the finite jump in each state variable is given by the so-called Rankine–Hugoniot (RH) relations [1], [2] that connect the upstream and downstream states of a shock.

These relations can be obtained from the conservation balance laws (11)–(13) by following the standard procedure given in [1] and employing the ideal gas equation of state. The standard Rankine–Hugoniot relations can be obtained as:

$$\begin{aligned} \rho_1\,\mathrm{u}_1 &= \rho_2\,\mathrm{u}_2, \\ \rho_1\,\mathrm{u}_1^2 + \rho_1\,\mathbf{R}\,\mathrm{T}_1 &= \rho_2\,\mathrm{u}_2^2 + \rho_2\,\mathbf{R}\,\mathrm{T}_2, \\ \rho_1\,\mathrm{u}_1^3 + 2\,\mathrm{c_p}\,\rho_1\,\mathrm{T}_1\,\mathrm{u}_1 &= \rho_2\,\mathrm{u}_2^3 + 2\,\mathrm{c_p}\,\rho_2\,\mathrm{T}_2\,\mathrm{u}_2. \end{aligned} \tag{14}$$

The modified Navier–Stokes equations, for the one-dimensional stationary shock flow configuration reduced to:

$$\frac{\mathrm{d}}{\mathrm{dx}}\left[\rho\,\mathrm{u}\right] = 0, \qquad \frac{\mathrm{d}}{\mathrm{dx}}\left[\rho\,\mathrm{u}^2 + \mathrm{p} + \Pi\right] = 0, \tag{15}$$

$$\frac{\mathrm{d}}{\mathrm{dx}}\left[\rho\,\mathrm{u}\left(\frac{1}{2}\,\mathrm{u}^2 + \mathrm{c_p}\,\mathrm{T}\right) + \Pi\,\mathrm{u} + \mathrm{q}\right] = 0. \tag{16}$$

Integration of the eqns (15)–(16) leads to:

$$\rho\,\mathrm{u} = \mathrm{m}_0, \qquad \rho\,\mathrm{u} + \rho\,\mathbf{R}\,\mathrm{T} + \Pi = \mathrm{p}_0, \tag{17}$$

$$\rho\,\mathrm{u}\left(\mathrm{c_p}\,\mathrm{T} + \frac{\mathrm{u}^2}{2}\right) + \Pi\,\mathrm{u} + \mathrm{q} = \mathrm{m}_0\,\mathrm{h}_0, \tag{18}$$

where $\mathrm{m}_0, \mathrm{p}_0$ and h_0 are integration constants which represents the mass flow rate, the stagnation pressure and the stagnation specific enthalpy, respectively, and their values can be obtained using the well-known Rankine–Hugoniot conditions (14). In order to solve the eqns (17) and (18), it is convenient to work with its dimensionless form. We use the following set of dimensionless variables based on the upstream reference states (denoted with subscript 1) as in Reese et al. [5], Reddy and Dadzie [17], and Dadzie and Reddy [22]:

$$\overline{\rho} = \frac{\mathrm{c}_1^2}{\mathrm{p}_1}\rho = \frac{\gamma}{\rho_1}\rho, \quad \overline{\mathrm{u}} = \frac{\mathrm{u}}{\mathrm{c}_1}, \quad \overline{\mathrm{T}} = \frac{\mathbf{R}}{\mathrm{c}_1^2}\mathrm{T}, \quad \overline{\mathrm{p}} = \frac{\mathrm{p}}{\mathrm{p}_1}, \quad \overline{\mathrm{x}} = \frac{\mathrm{x}}{\lambda_1}, \quad \overline{\mu} = \frac{\mu}{\mu_1}, \tag{19}$$

where λ_1 is the upstream mean free path which is a natural choice for a characteristic length-scale as changes through the shock occur due to few collisions and $\mathrm{c}_1 = \sqrt{\gamma\,\mathbf{R}\,\mathrm{T}_1}$ being the adiabatic sound speed. The upstream mean free path can be expressed as a function of reference state variables: $\lambda_1 = \lambda_0\mu_1/\rho_1\,\mathrm{c}_1$, with $\lambda_0 = (16/5)\,\sqrt{2\,\pi/\gamma}$. Dimensionless forms of transport coefficients $\overline{\kappa}$ and $\overline{\kappa}_\mathrm{m}$ are:

$$\overline{\kappa} = \frac{\gamma}{(\gamma-1)\,\mathrm{Pr}}\overline{\mu} \quad \text{and} \quad \overline{\kappa}_\mathrm{m} = \kappa_{\mathrm{m}_0}\frac{\overline{\mu}}{\overline{\rho}}, \tag{20}$$

with the Prandtl number, Pr, equals to $2/3$ for the case of a monatomic gas.

It is well-known that the viscosity and temperature relation has a noticeable effect on the shock wave structure. Here we adopt the generally accepted temperature-dependent viscosity power law [6], [16]: $\mu \propto \mathrm{T}^\mathrm{s}$ or $\mu = \alpha\,\mathrm{T}^\mathrm{s}$, where α is a constant of proportionality taken to be γ^s and the power s for almost all real gases falling between $0.5 \leq \mathrm{s} \leq 1$, with the limiting cases, $\mathrm{s} = 0.5$ and $\mathrm{s} = 1$ corresponding to theoretical gases, namely, the hard-sphere and Maxwellian gases, respectively. In our simulations we use $\mathrm{s} = 0.75$ for a monatomic argon gas.

The nondimensionalized form of the integral conservation eqns (17) and (18) can then be obtained using the dimensionless quantities defined via eqns (19) and (20) as:

$$\overline{\rho}\,\overline{\mathrm{u}} = \overline{\mathrm{m}}_0, \qquad -\frac{1}{\lambda_0\,\mathrm{Ma}_1}\,\overline{\Pi} = \frac{\overline{\mathrm{T}}}{\overline{\mathrm{u}}} + \overline{\mathrm{u}} - \overline{\mathrm{p}}_0, \tag{21}$$

$$-\frac{(\gamma-1)}{\lambda_0\,\mathrm{Ma}_1}\,\overline{\mathrm{q}} = \overline{\mathrm{T}} - \frac{(\gamma-1)}{2}\overline{\mathrm{u}}^2 + (\gamma-1)\,\overline{\mathrm{p}}_0\,\overline{\mathrm{u}} - \overline{\mathrm{h}}_0, \tag{22}$$

where Ma_1 is the upstream Mach number defined as the ratio of the speed of the gas to the speed of sound through the gas, $\mathrm{Ma}_1 = \mathrm{u}_1/\mathrm{c}_1$. Expressions for the quantities $\overline{\mathrm{m}}_0$, $\overline{\mathrm{p}}_0$ and $\overline{\mathrm{h}}_0$ can be then obtained as,

$$\overline{m}_0 = \gamma\,\mathrm{Ma}_1, \quad \overline{\mathrm{p}}_0 = \frac{1}{\gamma\,\mathrm{Ma}_1}\left(1 + \gamma\,\mathrm{Ma}_1^2\right), \quad \overline{\mathrm{h}}_0 = 1 + \frac{(\gamma-1)}{2}\mathrm{Ma}_1^2, \tag{23}$$

and the expressions for the dimensionless shear stress ($\overline{\pi}$) and the heat flux ($\overline{q}$) are given by,

$$\overline{\Pi} = -\frac{4}{3}\overline{\mu}\,\frac{\mathrm{d}\overline{\mathrm{u}}}{\mathrm{d}\overline{\mathrm{x}}} - \frac{4}{3}\left(\frac{\gamma}{\lambda_0}\right)\frac{\overline{\mu}\,\overline{\kappa}_\mathrm{m}}{\overline{\rho}}\,\frac{\mathrm{d}^2\overline{\rho}}{\mathrm{d}\overline{\mathrm{x}}^2} + \frac{4}{3}\left(\frac{\gamma}{\lambda_0}\right)\frac{\overline{\mu}\,\overline{\kappa}_\mathrm{m}}{\overline{\rho}^2}\left(\frac{\mathrm{d}\overline{\rho}}{\mathrm{d}\overline{\mathrm{x}}}\right)^2, \tag{24}$$

$$\overline{\mathrm{q}} = -\overline{\kappa}\,\frac{\mathrm{d}\overline{\mathrm{T}}}{\mathrm{d}\overline{\mathrm{x}}} - \frac{\gamma}{(\gamma-1)\,\mathrm{Pr}}\,\overline{\kappa}_\mathrm{m}\,\overline{\mathrm{T}}\,\frac{\mathrm{d}\overline{\rho}}{\mathrm{d}\overline{\mathrm{x}}}. \tag{25}$$

We solve the final eqns (21) and (22) using a numerical scheme, namely, finite difference global solution (FDGS) technique developed by Reese et al. [5] with well-posed boundary conditions. For the specific details of FDGS scheme reader can refer to Reese et al. [5].

4 NUMERICAL RESULTS AND COMPARISON OF HYDRODYNAMIC FIELDS ACROSS THE SHOCK LAYER

We perform numerical simulations of stationary shock waves located at $\mathrm{x} = 0$ using FDGS scheme by considering a computational spatial domain of length $100\lambda_1$ covering $(-50\lambda_1, 50\lambda_1)$ with a step size equal to $\approx 0.05\lambda_1$. This domain is wide enough to contain the entire shock profile for weak shocks ($\mathrm{Ma}_1 \sim 1$) without altering its structure in a monatomic argon gas. We assume the constant κ_{m_0} in the molecular mass diffusivity κ_m to be 0.5 in all our present simulations and for this value of κ_{m_0} the system is linearly stable. To compare the shock structure profiles among the theoretical and experimental data, the position x has been scaled such that $\mathrm{x} = 0$ corresponds to a value of the normalized gas density $\rho_\mathrm{N} = (\rho - \rho_1)/(\rho_2 - \rho_1)$ equals 0.5. Other hydrodynamic field, namely, the velocity profiles are normalised via: $\mathrm{u}_\mathrm{N} = (\mathrm{u} - \mathrm{u}_2)/(\mathrm{u}_1 - \mathrm{u}_2)$. Fig. 2(a) and (b) shows the comparison of the normalised velocity profiles obtained from the classical and the present modified Navier–Stokes equations for $\mathrm{Ma}_1 = 1.55$ and $\mathrm{Ma}_1 = 4$, respectively. As the flow varies from supersonic to subsonic across the shock, the velocity is maximum/high at the upstream part of the shock, decreases through the shock and attains its smallest value at the downstream part of the shock. The velocity profiles obtained from the modified NS model are more diffusive than the classical NS profile at both upstream and downstream part of the shock which is evident from Fig. 2.

4.1 Density profiles across the shock

Experimental data exist for monatomic argon gas density variations across shock layer. We take a detailed comparison of density field across the shock with experimental results

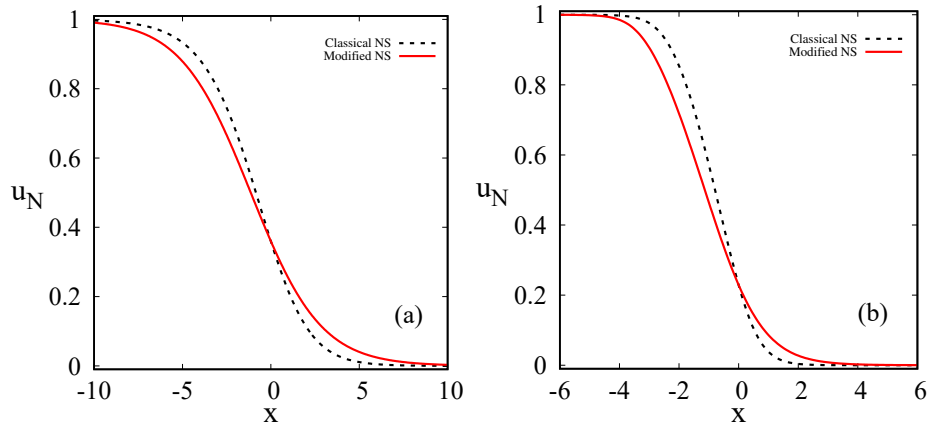

Figure 2: Variation of normalized velocity (u_N) profiles in Ar shock layer: for (a) $Ma_1 = 1.55$; and (b) $Ma_1 = 4$.

of Alsmeyer [13] and also with the classical Navier–Stokes equations. Fig. 3 show the normalized density ρ_N profiles through an argon shock wave as predicted by the modified Navier–Stokes and the classical Navier–Stokes equations compared with the experimentally measured density data. Panels (a), (b), (c) and (d) of Fig. 3 correspond to upstream Mach numbers of $Ma_1 = 1.55, 2.05, 3.38$ and 3.8, respectively. In each panel: the dotted black lines represent solutions of the Navier–Stokes equations and the red lines represent solutions by the modified Navier–Stokes equations. The filled blue circles represent the experimental data of Alsmeyer [13]. From panel (a) of Fig. 3 one observes that for the upstream Mach number of 1.55 the classical Navier–Stokes is able to predict well the upstream part of the shock layer in comparison with the experimental data but completely fails to predicts the downstream part of the shock layer. The modified Navier–Stokes equations produce good agreement with the experimental data with a small disparity at the upstream part of the shock layer and is more diffusive than the experimental data. The modified Navier–Stokes predictions for the normalized density profiles show excellent agreement with the experimental data for the upstream Mach number of $Ma_1 = 2.05, 3.38$ and 3.8, which is evident from panels (b)–(d) of Fig. 3. Overall, an excellent agreement between predictions of the modified Navier–Stokes equations and the experimental data of Alsmeyer [13] is found for weak shocks ($Ma_1 \sim 1$) to moderate strong shocks ($Ma_1 \sim 4$), which is seen in Fig. 3.

4.2 Shock macroscopic parameters: shock thickness and density asymmetry

We discuss in this section two important parameters, namely, shock thickness L_ρ and density asymmetry factor Q_ρ which are often used to characterize the shock wave properties instead of comparing full shock wave profiles. These two shock macroscopic parameters are defined based on shock density profiles. The usual shock thickness or width L_ρ is defined as (Greenshields and Reese [6], Reddy and Alam [7], [8], Gilbarg and Paolucci [10], Pham-Van-Diep et al. [12] and Alsmeyer [13]):

$$L_\rho = \frac{\rho_2 - \rho_1}{|\max(\frac{d\rho}{dx})|}, \tag{26}$$

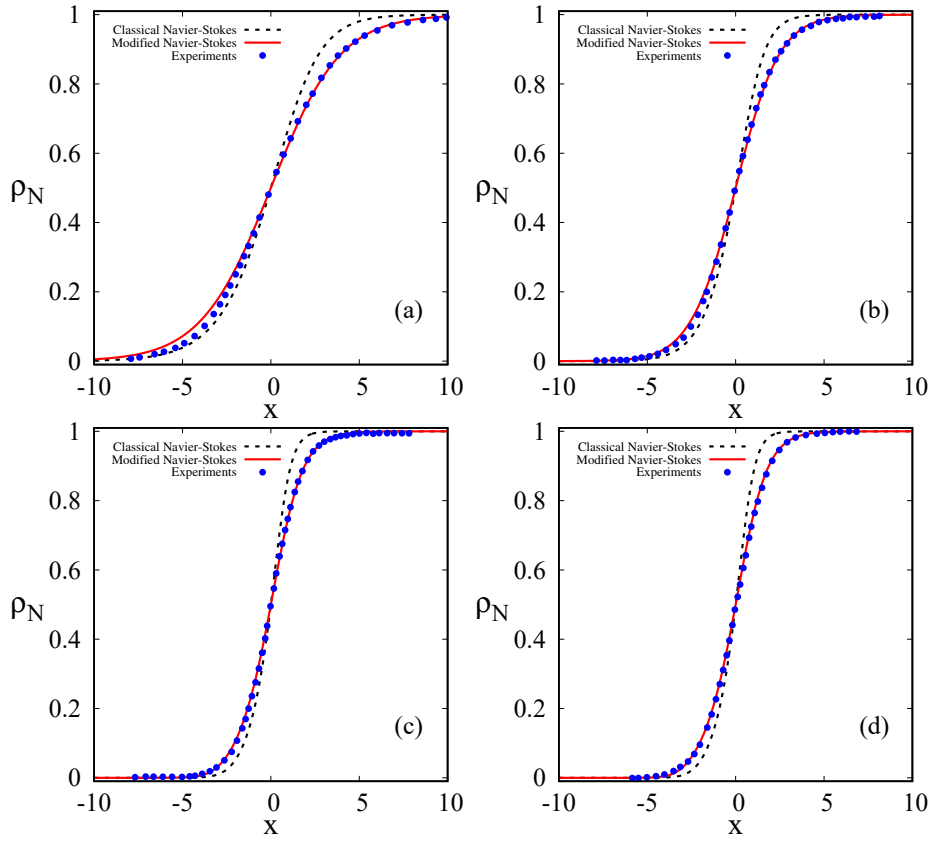

Figure 3: Variation of normalized density (ρ_N) profiles in Ar shock layer: for (a) $\mathrm{Ma}_1 = 1.55$; (b) $\mathrm{Ma}_1 = 2.05$; (c) $\mathrm{Ma}_1 = 3.38$; and (d) $\mathrm{Ma}_1 = 3.8$.

and is based on the density profile and depends mainly on the central part of the shock wave. Note that from the definition of L, one can infer that it has a linear dependence on the density difference between the upstream and downstream states and inversely proportional to a slope corresponding to the maximum density gradient. In general, the non-dimensional inverse shock thickness $\delta = \lambda_1/\mathrm{L}_\rho$ is used instead of shock thickness L_ρ to compare computational results with experiments as it possesses an important feature that is, it represents actually the Knudsen number of the shock structure flow problem.

In Fig. 4, the prediction of the modified Navier–Stokes equations (red line with filled rhombus) for reciprocal shock thickness (δ) as a function of upstream Mach number (Ma_1) are compared with the theoretical results from Burnett equations [16] (double dot dashed line), a second-order continuum equations of Paolucci and Paolucci [23] (dash dot line) along with the Alsmeyer experimental data (open and filled circles) and also with the DSMC data (filled squares). Predictions from the classical Navier–Stokes with $s = 0.75$ (see black dotted line) are also presented for the sake of completeness. From Fig. 5, one can observe that the classical Navier–Stokes equations with $s = 0.75$ predict the higher reciprocal shock thickness than the measured values over the entire Mach number range presented. In other

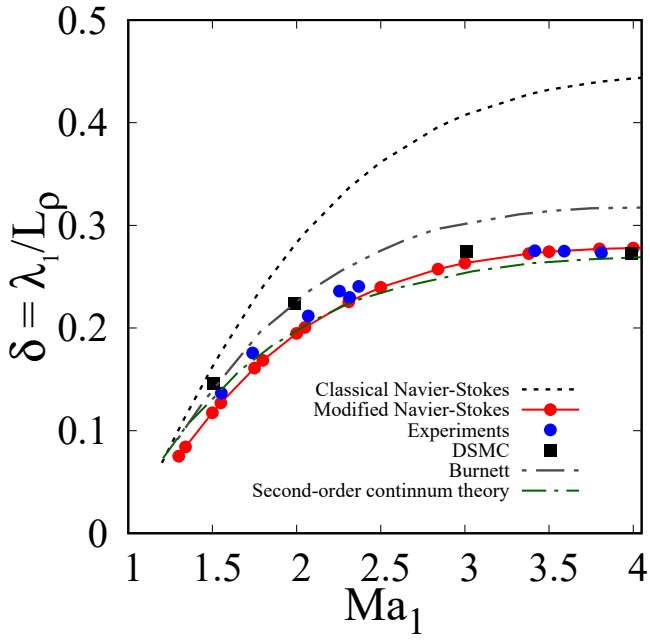

Figure 4: Variation of the dimensionless inverse shock thickness (δ) verses upstream Mach number Ma_1. Line with dot (red) represent modified Navier–Stokes solution with $\kappa_{m_0} = 0.5$ and $s = 0.75$, dashed line (black) shows present solutions of the NS with $s = 0.75$ using FDGS technique, results from Burnett theory and DSMC [16], second-order continuum theory [23] and experiments [13] are superimposed.

words we can say that the classical Navier–Stokes equations predicts very small values for the shock thickness (L_ρ). While the predictions from the modified Navier–Stokes equations with $s = 0.75$ is found to follow very closely the experimental results of Alsmeyer [13] (see filled blue circles). It can be seen that the predictions of the modified NS equations show a close reasonable agreement with the DSMC results of Lumpkin and Chapman [16] at all upstream Mach numbers ranging from $\mathrm{Ma}_1 = 1.55$ to 4. Some deviations from the Alsmeyer experimental results are observed in Burnett and second-order continuum model of Paolucci and Paolucci [23] which is evident from Fig. 4. Overall, judged by the inverse shock thickness, it has been found from Fig. 4 that the modified Navier–Stokes model gives good agreement with the experimental results of Alsmeyer [13] and a reasonable good agreement with the DSMC results [16]. Furthermore, the inverse shock thickness predictions of the modified NS equations showed improvement over the Burnett and the second-order continuum models.

A second important shock macroscopic parameter called the density asymmetry factor Q_ρ can be used to describe the actual shape of the shock structure as it measures skewness of the density profile relative to its midpoint [6]. The shock asymmetry, Q_ρ, is defined based on the normalized density profile, ρ_N, with its centre, $\rho_\mathrm{N} = 0.5$, located at $\mathrm{x} = 0$, as

$$\mathrm{Q}_\rho = \frac{\int_{-\infty}^{0} \rho_\mathrm{N}(\mathrm{x})\,\mathrm{dx}}{\int_{0}^{\infty} [1 - \rho_\mathrm{N}(\mathrm{x})]\,\mathrm{dx}}. \tag{27}$$

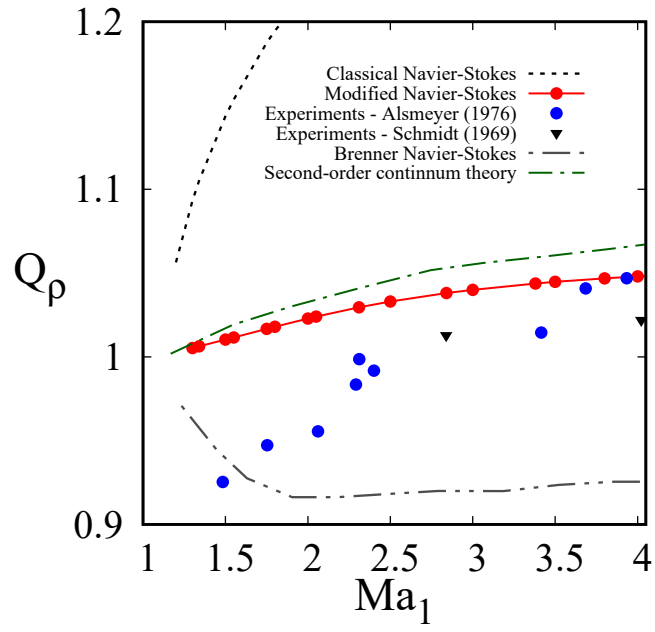

Figure 5: Variation of density asymmetry or shape factor (Q_ρ). Line with dot (red) represent modified Navier–Stokes solution with $\kappa_{m_0} = 0.5$ and $s = 0.75$, dashed line (black) shows present solutions of the NS with $s = 0.75$ using FDGS technique, results from Brenner Navier–Stokes [6], second-order continuum theory [23] and experiments [13], [14] are superimposed.

From eqn (27) it is clear that, a symmetric shock wave profile will have a density asymmetry quotient of unity, while for realistic shock waves its value is around unity and asymmetric shock profiles are predicted in experiments for strong hypersonic shock waves for which Q_ρ is always grater than unity.

Predictions of the modified Navier–Stokes equations for the density asymmetry quotient Q_ρ compared with experimental data of Alsmeyer [13] and Schmidt [14] along with the other theoretical predictions from the classical Navier–Stokes, a second-order continuum theory of Paolucci and Paolucci [23] and Brenner Navier–Stokes equations [6] are shown in Fig. 5. One can observe that the classical Navier–Stokes equations predict an asymmetry quotient of more than unity (which means that the upstream part of the shock profile is more skewed than at the downstream) at all upstream Mach numbers and are far away from the experimental predictions. Brenner Navier–Stokes equations predict $Q_\rho < 1$ for all upstream Mach numbers studied. In contrast to the predictions of classical and Brenner Navier–Stokes, it is experimentally found and reported that the density profile has a significant asymmetry ($Q_\rho = 1 \pm 0.15$) at all upstream Mach numbers. The modified Navier–Stokes predicts an asymmetry quotient of around unity at low upstream Mach numbers and its value increases with shock strength which is evident from Fig. 5. It can be seen that the current modified Navier–Stokes and second-order continuum theory of Paolucci and Paolucci [23] are better in predicting reasonable density asymmetry factor at all upstream Mach numbers range studied here.

5 CONCLUSIONS

In this work we presented a numerical investigation into shock wave profile description in a monatomic gas using hydrodynamics models by identifying constitutive equations that provide better agreement for the parameters involved in the prediction. A detailed comparison between the predictions of the modified hydrodynamic equations with Alsmeyer's experimental data and DSMC data along with classical Navier–Stokes hydrodynamic solutions presented for upstream Mach number range 1.3 to 4. First, we focused our comparison for shock density profiles as accurate data from the experiments are available. Second, we showed the comparison of two well-known shock macroscopic parameters (inverse shock thickness and density asymmetry factor) with available experimental and DSMC data. Our analysis showed that the constitutive equations provide excellent quantitative agreement with experimental data as well as with DSMC data at all Mach numbers discussed and especially best in reproducing experimental trends for the shock density and inverse shock thickness profiles. In fact we conclude that the results are improvement upon those obtained previously in bi-velocity hydrodynamics and showed improvements over those obtained using equations from the extended hydrodynamic approach of kinetic theory. Further implications of these results as related to recently proposed recast Navier–Stokes equations are still to be investigated.

ACKNOWLEDGEMENTS

This research is supported by the UK's Engineering and Physical Sciences Research Council (EPSRC) under grant no. EP/R008027/1 and The Leverhulme Trust, UK, under grant Ref. RPG-2018-174.

REFERENCES

[1] Courant, R. & Friedrichs, K.O., *Supersonic Flow and Shock Waves*. Interscience: New York, 1948.
[2] Liepmann, H.W. & Roshko, A., *Elements of Gas Dynamics*. John Wiley & Sons, Inc.: New York, 1957.
[3] Grad, H., The profile of a steady plane shock wave. *Communications on Pure and Applied Mathematics*, **5**(3), pp. 257–300, 1952.
[4] Bird, G.A., *Molecular Gas Dynamics and the Direct Simulation of Gas Flows*. Oxford University Press, 1994.
[5] Reese, J.M., Woods, L.C., Thivet, F.J.P. & Candel, S.M., A second-order description of shock structure. *Journal of Computational Physics*, **117**(2), pp. 240–250, 1995.
[6] Greenshields, C.J. & Reese, J.M., The structure of shock waves as a test of Brenner's modifications to the Navier-Stokes equations. *Journal of Fluid Mechanics*, **580**, pp. 407–429, 2007.
[7] Reddy, M.H.L. & Alam, M., Plane shock waves and Haff's law in a granular gas. *Journal of Fluid Mechanics*, **779**, p. R2, 2015.
[8] Reddy, M.H.L. & Alam, M., Regularized extended-hydrodynamic equations for a rarefied granular gas and the plane shock waves. *Physical Review Fluids*, **5**, p. 044302, 2020.
[9] Von Mises, R., On the thickness of a steady shock wave. *Journal of the Aeronautical Sciences*, **17**(9), pp. 551–554, 1950.
[10] Gilbarg, D. & Paolucci, D., The structure of shock waves in the continuum theory of fluids. *Journal of Rational Mechanics and Analysis*, **2**(5), pp. 617–642, 1953.

[11] Narasimha, R., Das, P. & Lighthill, M.J., A spectral solution of the Boltzmann equation for the infinitely strong shock. *Philosophical Transactions of the Royal Society of London Series A, Mathematical and Physical Sciences*, **330**(1611), pp. 217–252, 1990.
[12] Pham-Van-Diep, G.C., Erwin, D.A. & Muntz, E.P., Testing continuum descriptions of low-Mach-number shock structures. *Journal of Fluid Mechanics*, **232**, pp. 403–413, 1991.
[13] Alsmeyer, H., Density profiles in argon and nitrogen shock waves measured by the absorption of an electron beam. *Journal of Fluid Mechanics*, **74**(3), pp. 497–513, 1976.
[14] Schmidt, B., Electron beam density measurements in shock waves in argon. *Journal of Fluid Mechanics*, **39**(2), pp. 361–373, 1969.
[15] Stokes, G.G., On the theories of the internal friction of fluids in motion, and of the equilibrium and motion of elastic solids. *Transactions of the Cambridge Philosophical Society*, **8**, pp. 287–319, 1845.
[16] Lumpkin, F.E. & Chapman, D.R., Accuracy of the burnett equations for hypersonic real gas flows. *Journal of Thermophysics and Heat Transfer*, **6**(3), pp. 419–425, 1992.
[17] Reddy, M.H.L. & Dadzie, S.K., Reinterpreting shock wave structure predictions using the Navier-Stokes equations. *Shock Waves*, **30**, pp. 513–521, 2020.
[18] Reddy, M.H.L., Dadzie, S.K., Ocone, R., Borg, M.K. & Reese, J.M., Recasting Navier–Stokes equations. *Journal of Physics Communications*, **3**(10), p. 105009, 2019.
[19] Stamatiou, A., Dadzie, S.K. & Reddy, M.H.L., Investigating enhanced mass flow rates in pressure-driven liquid flows in nanotubes. *Journal of Physics Communications*, **3**(12), p. 125012, 2019.
[20] Dadzie, S.K., A thermo-mechanically consistent Burnett regime continuum flow equation without Chapman-Enskog expansion. *Journal of Fluid Mechanics*, **716**, p. R6, 2013.
[21] Brenner, H., Beyond Navier-Stokes. *International Journal of Engineering Science*, **54**, pp. 67–98, 2012.
[22] Dadzie, S.K. & Reddy, M.H.L., Recasting Navier-Stokes equations: Shock wave structure description. *AIP Conference Proceedings*, **2293**(1), p. 050005, 2020.
[23] Paolucci, S. & Paolucci, C., A second-order continuum theory of fluids. *Journal of Fluid Mechanics*, **846**, pp. 686–710, 2018.